Ber. Inst. Erdwiss. K.-F.-Univ. Graz	ISSN 1608-8166	Band 20/2	Graz 2014
PANGEO Austria	Graz, 14-19th September 2014		

Excursion 1

Geological Evolution of the Austroalpine Seckau Complex (Eastern Alps)

Magdalena Mandl[1], Walter Kurz[1], Stefan Pfingstl[1], Ralf Schuster[2], Christoph Hauzenberger[1] and Harald Fritz[1]

[1] Institut für Erdwissenschaften, Universität Graz, NAWI Graz, Heinrichstrasse 26 / Universitätsplatz 2, 8010 Graz, Austria

[2] Geologische Bundesanstalt, Neulinggasse 38, 1030 Wien

Introduction

The understanding of the tectono-metamorphic evolution of the Austroalpine Unit has made significant progress in the last few years (Schmid et al., 2004; Froitzheim et al., 2008). An essential key to reveal the tectonostratigraphy of Austroalpine nappes and the sequence of nappe emplacement was the analysis of the Alpine and pre-Alpine metamorphic evolution of distinct nappes (e.g., Schuster et al., 2004; Handy and Oberhänsli, 2004). Studies on these units, however, are rather unequally distributed. Strong emphasis was given on the investigation of units showing an Eo-Alpine high-grade metamorphic evolution including eclogite facies metamorphism, whereas the pool on structural, metamorphic, and geochronological data from other units is quite blank.

Thöni and Jagoutz (1993), Neubauer (1994), Plasienka (1995) and Froitzheim et al. (1996), Neubauer et al. (2000) among others, developed a picture where the Eo-Alpine metamorphism is related to the collision of the Austroalpine Unit with another continental fragment after closure of the Meliata Ocean to the south or southeast, the Austroalpine being in a lower plate position. An alternative model is given by Stüwe and Schuster (2010) where the formation of the Alpine orogenic wedge initiated at an intracontinental subduction zone which developed from a transform fault with a sinistral offset linking the Penninic (Alpine Tethys) Ocean and Neotethys (Meliata) Ocean in the Late Jurassic.

“Eo-Alpine” (as term for Early Cretaceous to early Late Cretaceous) deformation and metamorphism (e.g., Frank, 1987), however, is frequently taken uncritically to be related to Cretaceous nappe imbrication associated with general top-to-the-west emplacement. This concept, elaborated about 20-30 years ago, does actually not sustain critical review. Age data (e.g., Dal Piaz et al., 1995; Dallmeyer et al., 2008) and the sedimentary record (e.g., Frisch and Gawlick, 2003) suggest a large time span or time gap between the closure of the Triassic part of the Neotethys Ocean (Meliata oceanic realm) at ca. 160 Ma (Missoni and Gawlick, 2010) and classical “Eo-Alpine” ages dating high pressure metamorphism around 100-90 Ma (e.g., Thöni and Jagoutz 1992, 1993; Thöni et al., 2008). So the question arises whether a continuous process or distinct phases of convergence, collision, and subsequent extension formed the Austroalpine nappe pile. Additionally, many “classical” tectonic boundaries regarded as Alpine thrusts do not show any thrust-related fabrics although post-collisional extension was recognized to play a major role in Alpine orogeny (Ratschbacher et al., 1989).

Geological setting of the Austroalpine Unit

The Austroalpine Unit forms a complex nappe stack of crustal material which can be subdivided into a Lower Austroalpine and Upper Austroalpine Subunit (Schmid et al., 2004; Froitzheim et al., 2008). The recent Lower Austroalpine Subunit derived from the continental margin towards the Piedmont-Ligurian Ocean and was affected by extension during the Jurassic opening and by nappe stacking during Upper Cretaceous to Eocene closure of this oceanic realm, respectively. It is overlying the Penninic nappes of the Eastern Alps derived from the oceanic domain. The Upper Austroalpine Subunit represents a nappe pile which formed mainly during the Eo-Alpine event in the Early Cretaceous to early Late Cretaceous. Its lowermost part is the Silvretta-Seckau Nappe System consisting of a basement with a dominating Variscan metamorphic imprint and remnants of Permian to Lower Triassic cover sequence. The basement is dominated by paragneisses (partly magmatic) and orthogneisses with minor intercalations of micaschists, quartzites, amphibolites, hornblende bearing gneisses and local occurences of serpentinites and eclogites. Most of the amphibolites and orthogneisses developed from Cambrian to Ordovizian magmatic rocks and are interpreted to reflect pre-Cambrian to Ordovician collision, subduction and rifting processes (Neubauer, 2002). Additional some Carboniferous intrusions are present (Schermair et al., 1997). The magmatic inventory indicates Neoproterozoic to Ordovizian educt ages of the metasedimentary rocks. The medium to high grade imprint in these basement rocks occurred during the Variscan tectonometamorphic event (Neubauer et al., 1999). In the structurally deepest part of the westernmost element represented by the Silvretta Nappe also a Permian metamorphic overprint can be recognized (Schuster et al., 2004). The post-Variscan cover is best preserved in the Silvretta Nappe which is overlain by un-metamorphosed Permian to Triassic sediments in the Landwasser and Ducan synclines and a more or less stratigraphic contact to the Permomesozoic sequences of the Bajuvaric Nappe System (Nowotny et al., 1992; Nagel, 2006). Further to the east tectonically truncated sequences show an eo-Alpine greenschist facies overprint. They comprise only Permian metaconglomerates and metapelites as well as Lower Triassic quartzites. In the basement units the eo-Alpine imprint reaches Sub-greenschist to epidote-amphibolite facies conditions causing a retrograde overprint in most of the Variscan metamorphic rocks (Neubauer et al., 1995; Schuster et al., 2004; Hoinkes et al., 2010). Nappes of the Silvretta-Seckau Nappe System build up antiformal structures in the western (Schladminger Tauern) and eastern part (Seckauer Tauern) of the Niedere Tauern mountain ridge.

To the north the Silvretta-Seckau Nappe System is overlain by the nappes of the Greywacke zone, which consists of greenschist facies metamorphic Paleozoic sequences, and the Juvavic, Tirolic-Noric and Bajuvaric Nappe Systems. The latter form the Northern Calcareous Alps, mostly comprising unmetamorphosed to lowermost greenschist facies metamorphic Permian to Mesozoic sediments deposited on the shelf facing originally towards the Meliata Ocean, with the sequences of the Juvavic Nappe System representing the most distal shelf towards the oceanic basin.

To the south the Silvretta-Seckau Nappe System is overlain by the Koralpe-Wölz Nappe System which represents an Eo-Alpine metamorphic extrusion wedge (Schmid et al., 2004). Its Permian to Mesozoic cover was completely stripped off during an early phase of the Eo-Alpine orogenic event and it therefore consists exclusively of metamorphic basement nappes. To a various grade the individual nappes are affected by a Variscan, Permian to

Triassic HT/LP and an Eo-Alpine HP metamorphic overprint (Neubauer, 1999; Schuster et al., 2004).
The Ötztal-Bundschuh Nappe System shows a similar lithological composition as the Silvretta-Seckau Nappe System, but is positioned on top of the Koralpe-Wölz Nappe System. The overlying Drauzug-Gurktal Nappe System is made up of a Variscan metamorphic basement, anchizonal to greenschist facies Paleozoic metasedimentary sequences and by un-metamorphosed Permian to Triassic sediments (Rantitsch and Russegger, 2000). Within the Ötztal-Bundschuh and Drauzug-Gurktal Nappe Systems the Eo-Alpine metamorphic grade decreases upwards from epidote-amphibolite facies at the base to diagenetic conditions at the top of the nappe pile. In other words, the high-grade nappes of the Koralpe-Wölz Nappe System are sandwiched between nappes affected by rather medium to low-grade Eo-Alpine metamorphism.

Geology of the Seckau Complex

According to Schmid et al. (2004) and Froitzheim et al. (2008), the Seckau Complex forms part of the Seckau Nappe which is part of the Silvretta-Seckau Nappe System (Fig. 1, 2). The Silvretta Nappe forms a more or less triangle shaped area extending in the north from the Bösenstein massif and Seckauer Tauern in the eastern part of the Niedere Tauern to the Fischbacher Alps over nearly 100 km. There it is cut off by the sinistral, east-west trending Trofaiach fault. Its continuation is represented by the Troiseck Floning Nappe (Neubauer, 1988). The southern edge is at Ammeringkogel in the northern part of the Koralpe mountain ridge (Becker, 1979). The north south extension is about 50 km.
The nomenclature used in literature for the crustal piece referred as Seckau Nappe in here is quite complicated and confusing. Until the 70ies of the past century it is attributed to the so called Muriden unit in contrast to the overlying Koriden unit. This was however a local subdivision which was never extended over the whole Austroalpine Unit.
Names used for the area of the Bösenstein massiv and the Seckauer Tauern, which is dominated by orthogneisses, paragneisses and migmatic paragneisses (Metz, 1976) were “Seckauer Gneis“ (Schmidt, 1921, p. 103 ff), „Seckauer Masse“, „Seckauer Massiv“ (Tollmann, 1977), „Kristallin der Seckauer Tauern“ (Metz, 1980) and „Seckauer Kristallin“ (Scharbert, 1981, Tollmann, 1977, p. 287). To favour is the term Seckau Complex (Faryad & Hoinkes, 2001, Gaidies et al., 2006) because it matches recent lithostratigaphic standards (GeoSciML).
For the eastern continuation „Mugel-Rennfeldzug“ (Schwinner, 1951, S. 110; Metz, 1971, S. 56; Tollmann, 1977, S. 222) and „Rennfeld Mugel Kristallin“ (Neubauer, 1988) can be found. In the southern part two units have been distinguished. A lower Ammering-Komplex (Flügel and Neubauer, 1984 after „Ammeringserie bzw. Gneiskomplex“ in Becker, 1980) formed by biotite-plagioclase paragneisses and some orthogneis intercalations is overlain by the Speik-Komplex (Flügel and Neubauer, 1984, after „Speikserie bzw. Amphibolitkomplex“ in Becker, 1980) dominated by amphibolites with some ultramafic rocks and an eclogite at Hochgrössen mountain. However, the individual complexes are not well defined and their boundaries are not clear. The overlying Permian to Lower Triassic metasediments are summarized as Rannach-Formation (Flügel and Neubauer, 1984, after “Rannachserie” from Metz, 1967). It has to be mentioned that the term Rannach-Formation is problematic because there is a Rannach-Group (Flügel and Neubauer, 1984) defined in the nappes of the Graz Paleozoic just 30 km to the southeast.

In the north the Rannach-Formation is overlying the Seckau Complex with a northward dip, whereas in the south the Spike Komplex is the uppermost element. Further, the Gaal Zone (Metz, 1971, "Gaaler Schuppenzone") mainly composed of the Spike Complex and overlying Permian to Lower Triassic metasediments is tectonically overlying the northwesternmost part of the Seckau Nappe in the Bösenstein area.

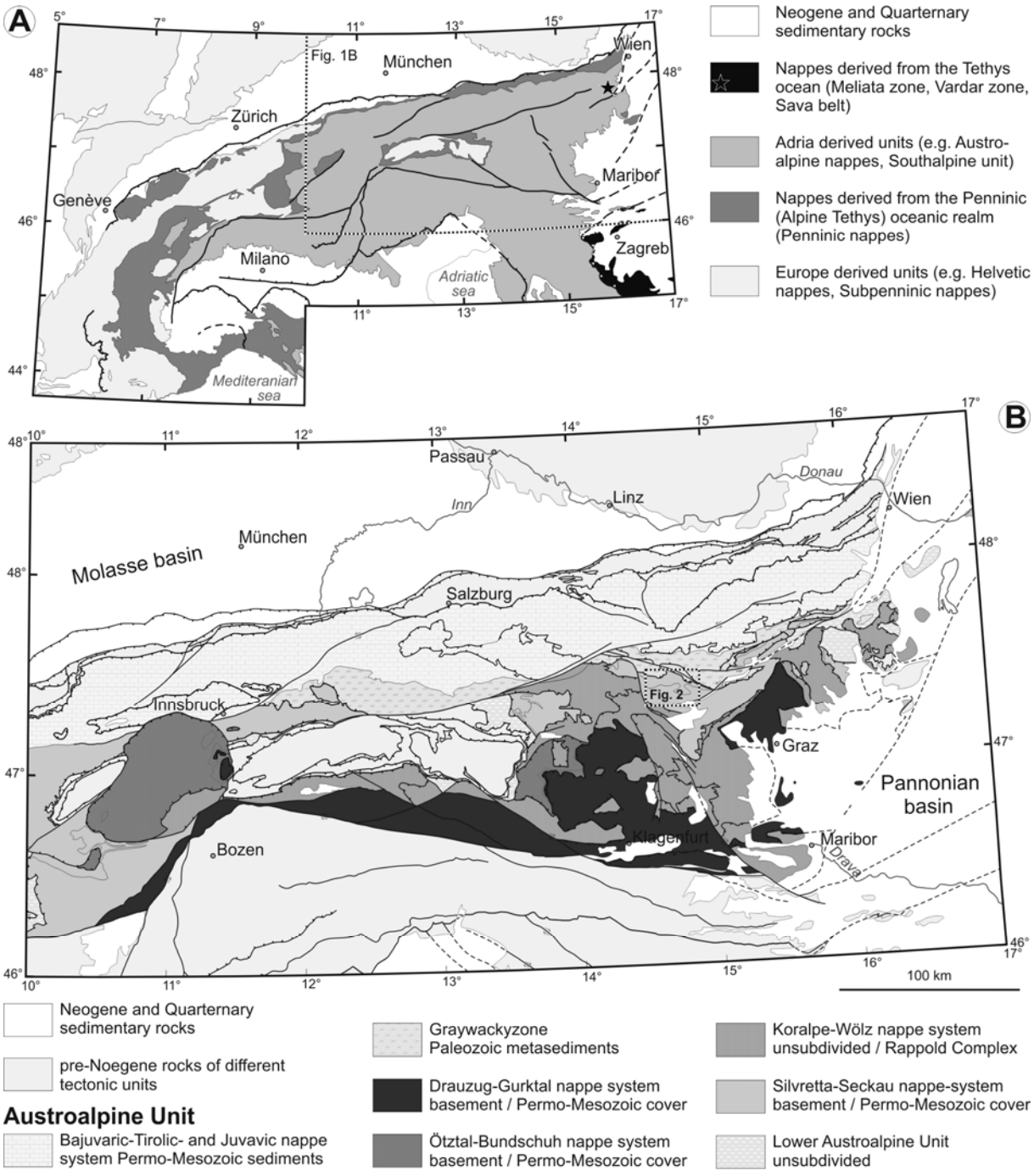

Figure 1: Overview maps (A) showing the paleogeographic origin of the main tectonic units of the Alps, and (B) the tectonic subdivision of the Austroalpine unit based on Schmid et al. (2004).

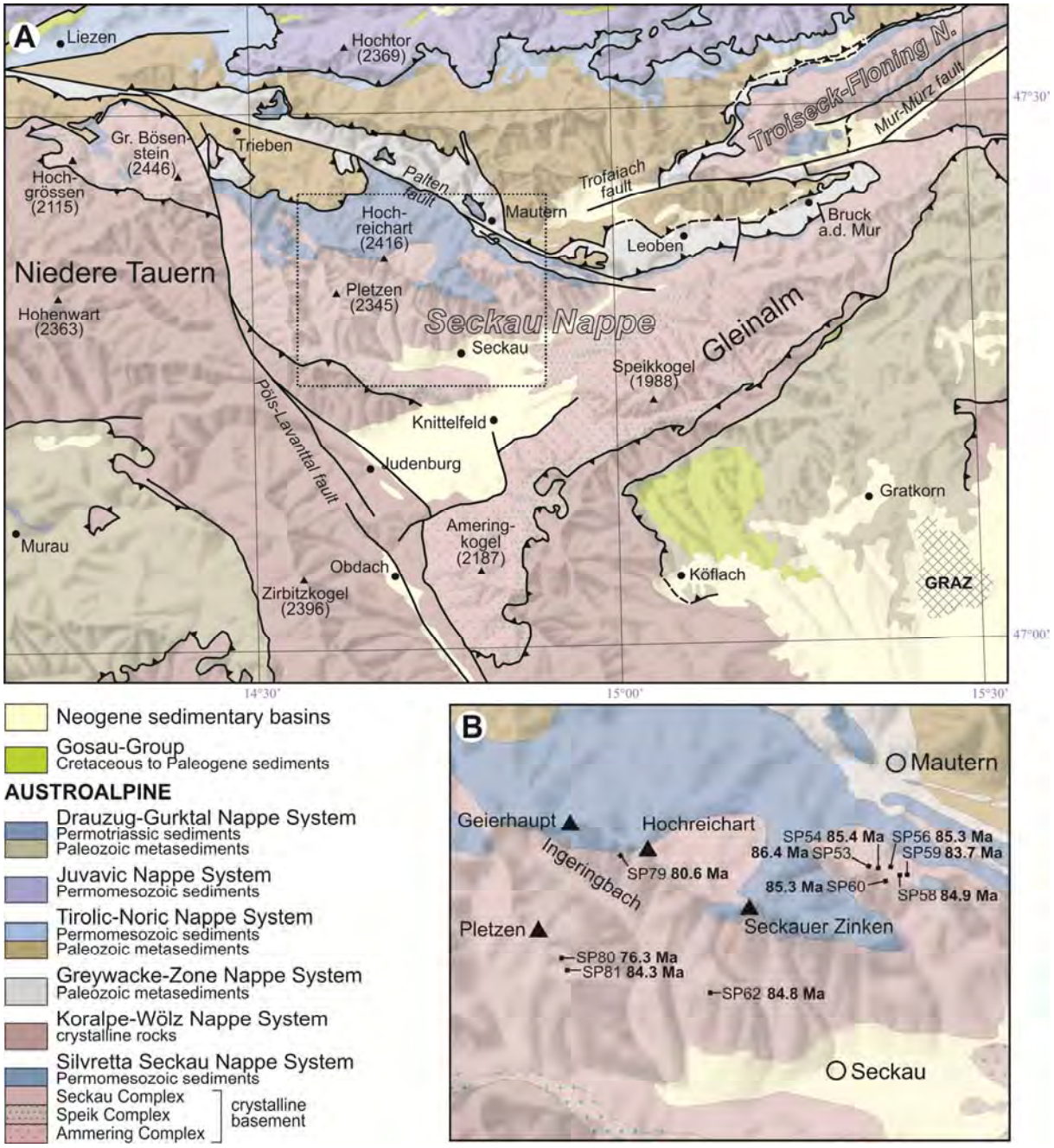

Figure 2: (A) Geological map of the study area in the Seckauer Tauern, based on Metz (1967, 1979), Flügel and Neubauer (1984) and Schubert et al. (2009). (B) Enlargement of the sampling area with sites of samples and the revealed Rb-Sr isochron ages.

As mentioned before the Seckau-Complex is formed by orthogneisses, paragneisses and migmatic paragneisses. The orthogneisses and augen gneisses derived from tonalites, granodiorites as well as granites. In general these units form a coherent suite of I-type granitoids (Schermaier et al., 1997; Pfingstl, 2013). A-type, and transitional S- and I- type granitoids are represented to minor extent. Based on Rb-Sr whole rock (~ 350 Ma) and white mica ages (~330 Ma) and the contact to the Permomesozoic metasediments the orthogneisses are thought to have formed during the Variscan tectonometamorphic event (Scharbert, 1981). An additional Rb-Sr whole rock age of 432 +/- 16 Ma argues for a pre-

Variscan, possibly Ordovician intrusion age. However, to clarify the ages of the individual intrusive bodies modern zircon ages are necessary.
In the map of Metz (1967) the Rannach-Formation ("Rannach Serie") in the northern part of the Seckauer Tauern comprises Permian metaconglomerates, metapelites derived from fine grained clastic sediments and some carbonatic intercalations. Lower Triassic thin bedded greenish quartzites occur in the north within a window near to the village Wald am Schoberpass below the nappes of the Greywacky Zone. In the eastern continuation the Permian Metasediments are often referred as "Alpine Verrucano", whereas the Lower Triassic quartzites represent the Semmering quartzite.
Permian to early Mesozoic (meta-)sedimentary units except those of the Northern Calcareous Alps and the Drau Range were summarized as Central Austroalpine Mesozoic (CAM) (e.g. Tollmann, 1977). They are widely dispersed on most of the Austroalpine nappe systems. Prominent examples for CAM are the Brenner Mesozoic in the west and the Stangalm, Thörl and Rannach Permo-Mesozoic units to the east of the Tauern Window, respectively. Most of the clastic Permian to Lower Triassic sequences of CAM have minor thicknesses between few meters (Brenner, Stangalm units) to at maximum 100 meters (Thörl unit) (e.g., Schnabel, 1980). An exception is the Rannach-Formation (Metz, 1976) with up to 1000 meters thickness.
The metamorphic conditions in the Seckau Nappe show a slight increase towards the south. In the north the transgressive Permian to Lower Triassic metasediments (Rannach-Formation) are characterised by the assemblage muscovite + chloritioide + chlorite + quartz, indicating upper greenschist facies conditions (520°C at 0.9 GPa; Faryad and Honikes, 2001). In the Gleinalm area in the south lower amphibolite facies conditions are expected from amphibolite assemblages including garnet + amphibole + plagioclase and intercalated micaschists with garnet, staurolite and kyanite.
Timing of the peak of eo-Alpine metamorphism in the Seckau nappe is not constrained with data and also for the cooling through greenschist facies conditions the data are scarce. Three Rb-Sr biotite ages in the range of 70 to 77 Ma (Scharbert, 1981). Unexpected high fission track ages were described by Hejl (1997). Orthogneiss samples from the summit and valley areas of the Seckau Tauern yielded apatite fission track ages of ca. 60 Ma and 44 Ma, respectively. These fission track data indicate that after fast denudation during Late Cretaceous times the Seckau Nappe stayed at nearly constant temperature in the order of 80°C until the late Oligocene, followed by a phase of faster cooling, and a phase of slow cooling during Miocene times. The fission track data exclude any post-Cretaceous metamorphic overprint within the Seckau Nappe. During the whole Cenozoic the highest portions of the Seckau Nappe therefore resided at a depth of less than 3000 meters at temperatures much cooler than the conditions of anchimetamorphism (Hejl 1997).

Geochemical data of granitoides

The mainly foliated samples were recovered from two localities, namely in the Untere Bodenhütte (in reddish symbols in Fig. 3) and Ingering Gaal area (in bluish color in Fig. 4). The geographic location of the samples and their lithological / geochemical classification are given in Table 1, analytical data in Table 3 (Appendix).

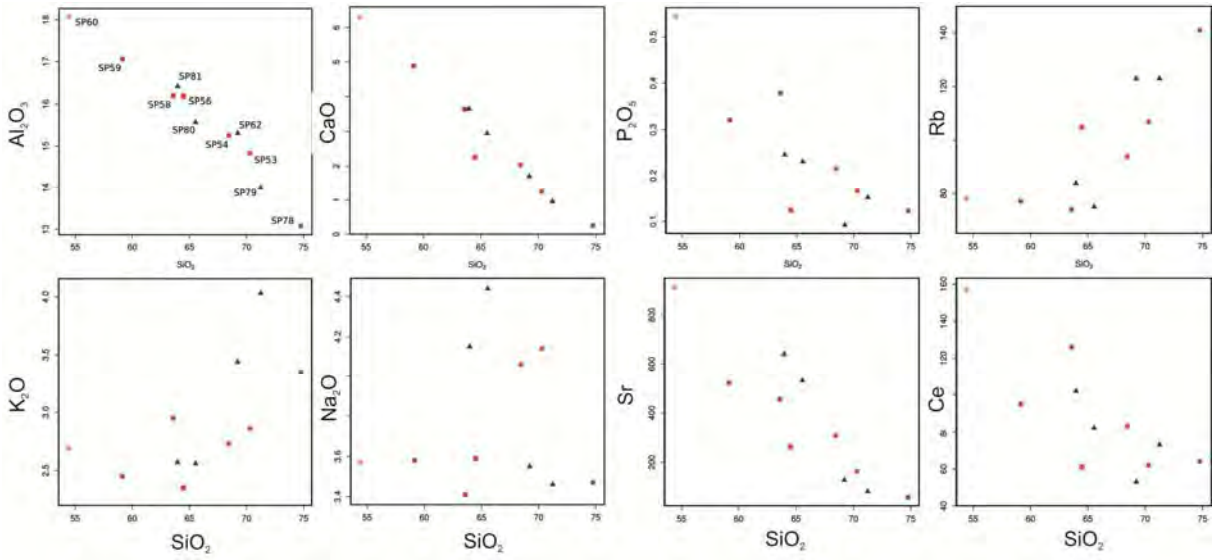

Figure 3: Total alkali (Na2O + K2O) against SiO2 classification diagram after Middlemost 1994. Symbols in reddish/magenta colour indicate samples from the "Untere Bodenhuette", samples in blue are from the "Ingering Gaal" area.

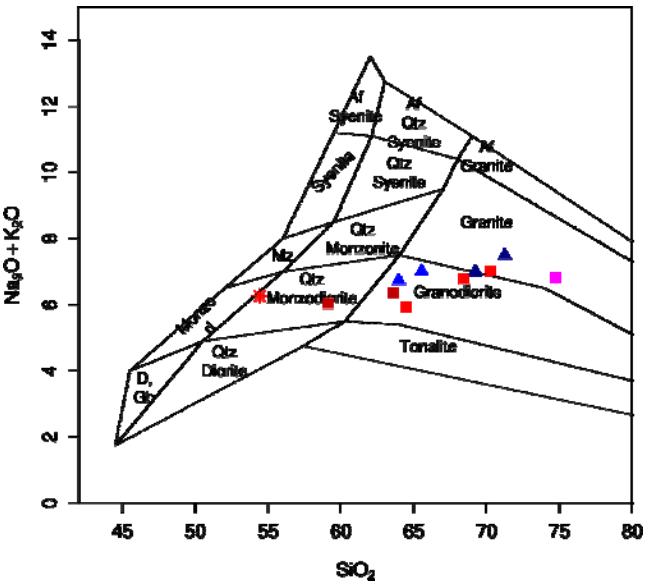

Figure 4. Harker diagrams with selected major and trace elements. The porhphyric samples (dark red) have low SiO_2 values but high in CaO, P_2O_5, Sr and Ce. The S-type orthogneiss samples SP62 and SP79 are relatively enriched in SiO_2, K_2O and Rb, while low in CaO, Na_2O, P_2O_5, Sr and Ce.

Samples from the Untere Bodenhütte area include two porhphyric and only weakly foliated samples (SP58, SP59). They have a distinct appearance with low SiO_2, Na_2O and Rb concentrations but show the highest CaO, P_2O_5, Sr, and Ce contents. One sample (SP78), which did not contain biotite and thus was not dated, contained muscovite and geochemical data are plotted for comparison in Figure 4. This sample shows slightly different chemical features and contains the highest SiO_2 values of all samples with 74.8 wt.%. From the Ingering Gaal area four samples were taken. Two samples display higher SiO_2, K_2O and Rb while CaO, P_2O_5, Sr, and Ce values are very low. Based on geochemical and Sr isotope data both samples were identified to belong to a granitic suite with S-type affinity. However, most analyzed samples can be geochemically classified as I-type granites with respect to Chappel and White (1974, 2001) (Pfingstl 2013) (Table 1). Sample SP60 from the Feistritz valley has been identified as metamorphosed mafic dike. Following the classification by Middlemost

(1994) by application of the TAS diagram for plutonic rocks samples SP53, SP62, SP79, and SP78 can be classified as granites, and SP54, SP56, SP58, SP80 and SP81 as granodiorites (Figure 4). Only sample SP59 falls into the quartz monzodiorite field. The metamorphosed mafic dike SP60 has a basaltic trachyandesite/quartz-monzodiorite composition.

Geochronological data

The results of geochronological analysis are summarized in Table 2 (Appendix), related Rb-Sr biotite ages are displayed in Figure 2 and related isochrons are given in Figure 5. The investigated biotites show brown to yellowish-brown pleochroism. Some separated from orthogneisses show typical rutile exolutions (“Sagenitgitter”), indicating higher Ti-contents of the primary magmatic biotites. Within the eastern part of the investigated area ages range from 84.9 to 86.4 Ma. Taking into account the standard deviations (Table 2), these ages are more or less identical within error. A similar age of 84.8 Ma (SP62) has also been observed from the southern part of the investigated area. An age from the Hochreichart (Fig. 2) yielding 80.6 Ma is significantly younger. In the western part of the area of investigation, west of the Ingering valley, two different ages were observed. An age of 84.3 Ma (SP81) is widely identical to the bulk of ages yielded in the eastern part, whereas an age of 76.3 Ma is significantly younger (SP80).
Calculation of an isochron including all whole rocks of granitic and granodioritic rocks results in an age value of 517±61 Ma with an initial isotopic ratio of 0.7045±0.0016.

Microstructures

Within the deeper levels of the Seckau Complex quartz is characterized by partly annealed fabrics. Equigranular grains generally show a polygonal shape (Fig. 6a). Quartz grains show grain sizes of 0.2 - 0.4 mm, the average grain size equals about 0.3 mm. Irregular and lobate grain boundaries are weakly developed; generally the grain boundaries are straight or slightly curved and form 120°- triple junctions. In places, the grains were subsequently affected by low-temperature deformation, and, therefore, show undulatory extinction.
Along the contact to the Rannach-Formation quartz grains are slightly elongated (Fig. 6b). Ribbon grains formed along shear bands. The quartz grains are characterized by undulatory extinction, the formation of subgrains, deformation lamellae and deformation bands, and by sutured, lobate, and bulged grain boundaries. Aggregates of fine-grained dynamically recrystallized grains (grain size ~ 0.05 - 0.1 mm) developed along shear bands due to secondary grain size reduction; bulging is assumed to be the main deformations mechanism.
Along the contact between the Seckau Complex and the Rannach-Formation both K-feldspar and plagioclase show high undulatory extenction, and, within domains along shear bands, curved twins. The feldspars are characterized by cataclastic deformation mechanisms, documented by the formation of extensional fractures and shear fractures (Fig. 6c). Extensional fractures are filled with quartz and calcite. Fragments confined by shear fractures were rotated towards the direction of shear that is accommodated by single and/or conjugate sets of shear bands. Along these shear bands (Fig. 6b) quartz is characterized by grain size reduction due to dynamic recrystallization. Biotite is aligned along these shear bands; within distinct domains biotite recrystallized and was newly formed. Additionally biotite is transformed to chlorite. In case of the occurrence of single sets the shear bands indicate a

top-to-the WNW sense of shear. Antithetic sets top-to-the ESE kinematics can be observed as well, but are developed to a lesser extent.

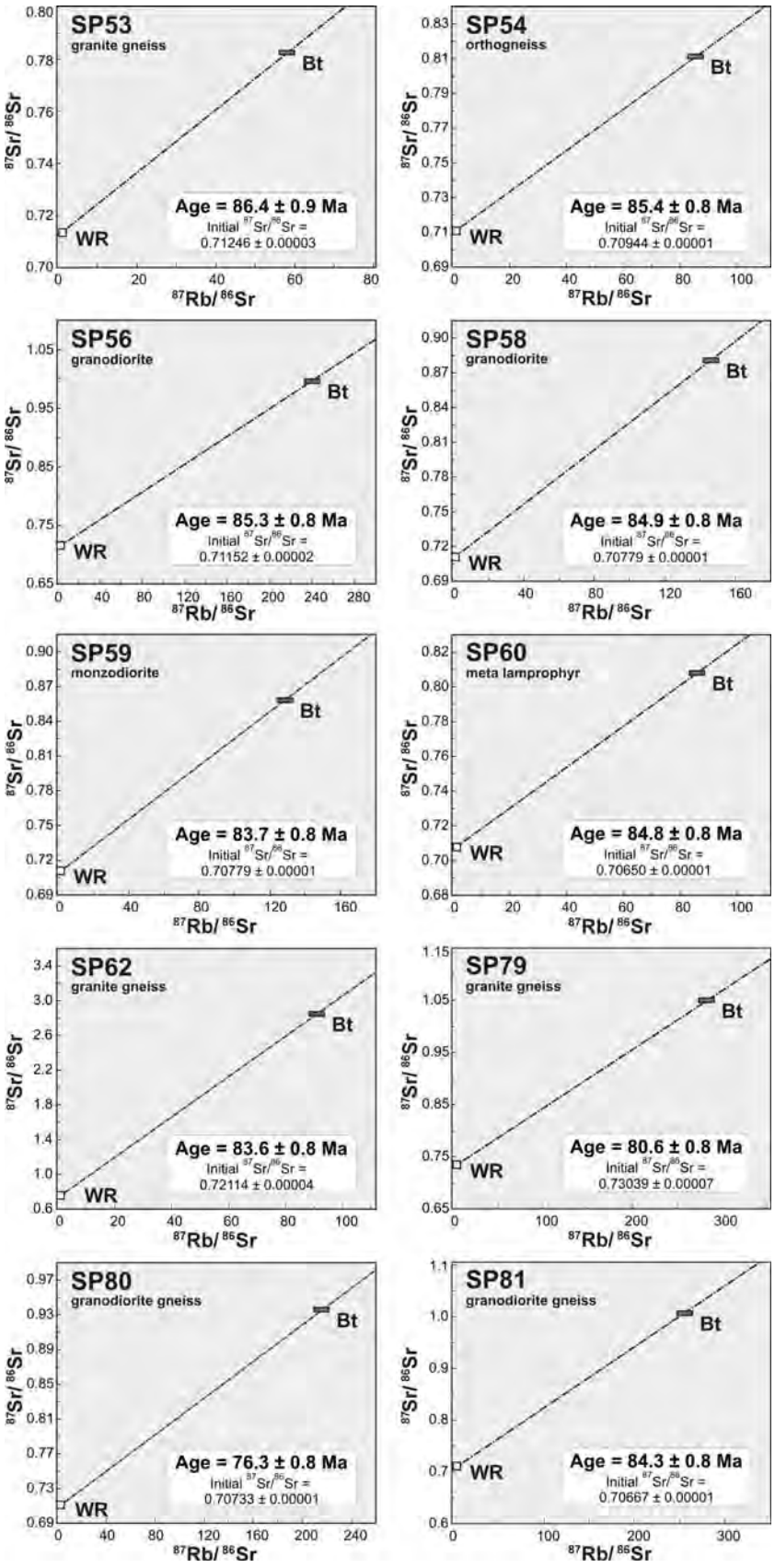

Figure 5: Selected tie line ages from orthogneisses of the Seckau Complex.

As feldspar is deformed by cataclastic deformation mechanisms, whereas quartz show deformation mechanisms of dislocation creep and bulging dynamic recrystallization we assume that the conditions of deformation along the Seckau Complex with the Rannach-Formation are in the range of 300°C to 400°C.

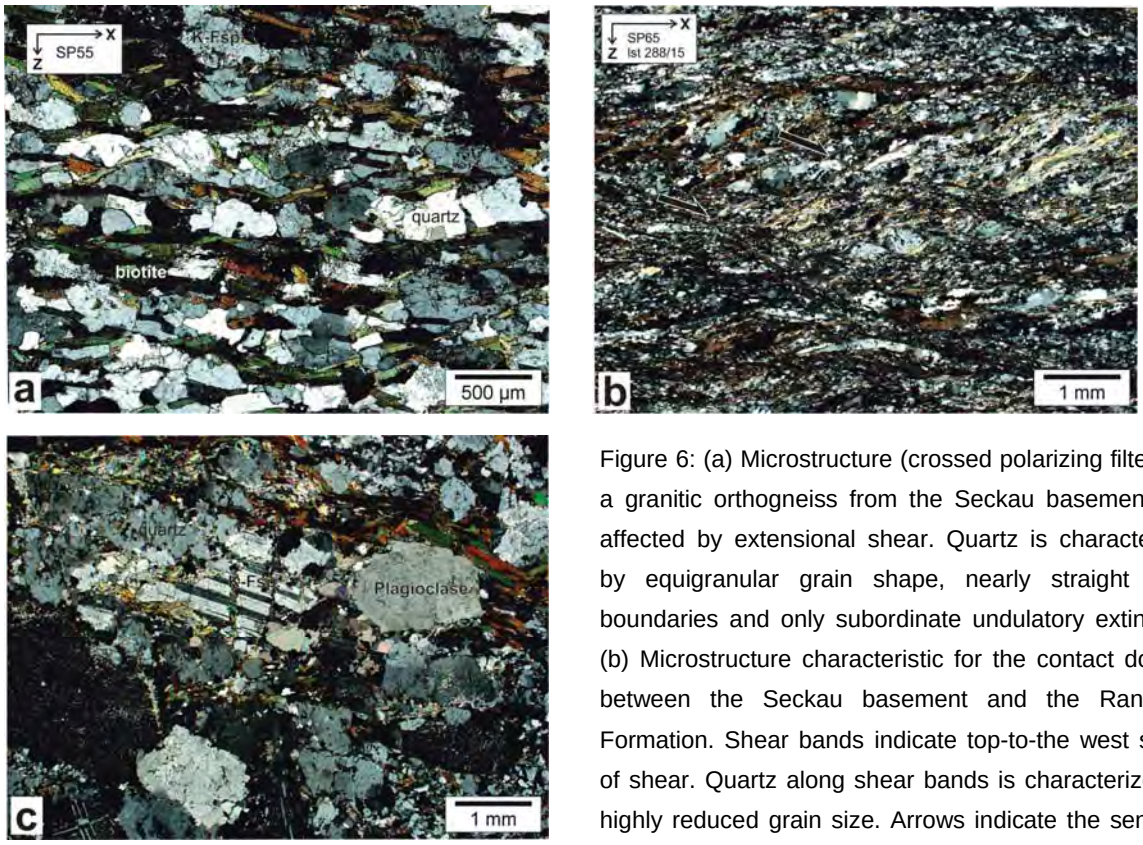

Figure 6: (a) Microstructure (crossed polarizing filters) of a granitic orthogneiss from the Seckau basement, not affected by extensional shear. Quartz is characterized by equigranular grain shape, nearly straight grain boundaries and only subordinate undulatory extinction. (b) Microstructure characteristic for the contact domain between the Seckau basement and the Rannach-Formation. Shear bands indicate top-to-the west sense of shear. Quartz along shear bands is characterized by highly reduced grain size. Arrows indicate the sense of shear.

(c) Microstructure of a granitic orthogneiss from the Seckau basement, immediately beneath the contact to the Rannach-Fomation. Quartz is characterized by undulatory extinction and formation of multiple subgrains, Feldspar is characterized by undulatory extinction, bent twins, and fracturing.

Alpine Evolution of the Seckau Complex

The Rb-Sr biotite age data range from 76 to 86 Ma, with eight samples showing ages between 84 and 86 Ma. A sample from Hochreichart mountain has an age of 80.6 Ma, another sample west of the Ingering valley yielded only 76.3 Ma. The latter seems to be exceptional as it is sampled only about 250 meters from sample SP81, which has an age of 84.3 Ma and as both samples showing a nearly identical mineralogical and chemical composition. It is obvious that both samples underwent the same cooling history and we attribute the small difference in age to a slight contamination by chlorite, grain size and/or weathering effects. According to Jäger (1979) Rb-Sr biotite-ages are interpreted to date cooling below 300±50°C. Therefore the investigated part of the Seckau Complex (Jäger, 1979) cooled down below ~300°C at about 85 Ma in the Santonian.

An isochron calculated from all investigated whole rock analyses will not represent a geological meaningful age because most probably the rocks do not represent a cogenetic magmatic suite and therefore their melts will not have equilibrated at a certain time. However, the isochron indicates a Phanerozoic crystallisation because for older ages the

initial isotopic ratio of the isochron, as well recalculations for the individual data points yield values >0.704 which are unrealistic for graniotic rocks on earth. This conclusion is in line with conclusions published by Scharbert (1981) and Schermaier et al. (1997).

Referring to microstructural observations, the contact between the Seckau Complex and the Rannach-Formation was strongly overprinted by the formation of distinct shear zones that are characterised by extensional fabrics. Kinematics is characterized by conjugate sets of top-to-the-WNW and top-to-the-ESE

A comprehensive view of the ages and structural observations presented in this study shows that deformation temperatures overlap with the range of Rb-Sr biotite closure temperature. Therefore we assume that top-to-the WNW extensional shearing is related to exhumation of the Seckau Nappe and caused cooling below 300±50°C at 85 Ma in the Late Cretaceous. This coincides with the formation of the Gosau sedimentary basins in the central Eastern Alps (Neubauer et al. 1995; Faupl and Wagreich, 2000).

The Rb-Sr biotite ages by Scharbert (1981), which are slightly younger have been measured on samples taken from the more southern part of the Seckauer Tauern and may indicate a trend to later cooling towards the south.

Ages from the Seckau Complex in the adjacent Gleinalm area in the southeast and from the Gaal Zone in the Bösenstein massif in the west give additional information. An $^{40}Ar/^{39}Ar$ amphibole age measured on an eclogite amphibolite of the Spike Complex of the Gaal Zone yielded about 390 Ma (Faryad et al., 2002). This pre-Alpine age survived because metamorphic conditions determined for the northern part of the Silvretta-Seckau Nappe System are around 500°C in the range of the closure temperature of the K-Ar isotopic system in amphibole (von Blanckenburg and Villa, 1988; von Blanckenburg et al., 1989). In contrast an $^{40}Ar/^{39}Ar$ age from the Speik Complex in the Gleinalm area yielded 95.4±1.2 Ma (Neubauer et al., 1995). This age reflects total reset of the K-Ar isotopic system in hornblende during eo-Alpine epidote-amphibolite facies metamorphism at 550-600°C at 0.9-1.0 GPa (Faryad and Hoinkes, 2003).

In the Gleinalm mountain range the Spike Complex is overlain by the Wölz and Rappold Complexes being parts of the Koralpe-Wölz Nappe System. $^{40}Ar/^{39}Ar$ muscovite ages from there are in the range of 84 to 87 Ma (Neubauer et al., 1995). These muscovite ages are in the range of the new Rb-Sr ages presented in this study. Despite the fact that the closure temperature of the Ar-isotopic system in white mica has been reported to be within a rather wider temperature range from ca. 350°C (Lips et al. 1998) to ca. 450 °C (Hames and Bowring, 1994; Kirschner et al., 1996) and ca. 500°C (Hammerschmidt and Frank, 1991; Hames and Cheney, 1997) and depend on grain-size, chemical composition and cooling rate, it is higher than those for Rb-Sr in biotite (Jäger, 1979; 300±50°C). This indicates earlier cooling of the Seckau Nappe below 350°C within the Seckauer Tauern than in the Gleinalm mountain range.

Fission track data from the Gleinalm mountain range measured on sphene, zircon and apatite yielded ages of ca. 94 Ma, 65 Ma, and 34 Ma, respectively (Neubauer et al., 1995; Dunkl et al., 2005). The fission track ages therefore support the trend with earlier cooling in the Seckauer Tauern with respect to the Gleinalm mountain range: The zircon fission track age of 65 Ma representing cooling below partial annealing zone representing < 240°C (e.g., Wölfler et al., 2010) is just slightly older than the apatite fission track ages from the Seckauer Tauern yielding 60-44 Ma (Hejl, 1997). The latter indicates that the northern part of the Seckau Complex cooled below the apatite fission track partial retention zone (120° - 60°C;

Green et al., 1986; Wolf et al., 1996) in Oligocene times. The apatite fission track age from the Gleinalm is 34 Ma (Dunkl et al., 2005) and indicates cooling 25-30 Ma later than in the north.

Compared to the cooling path of the basement rocks in the Seckau Tauern described above, cooling of the adjacent Gleinalm mountain range southeast of the Seckau Tauern, appears to be more continuous (Fig. 7). The data set form the Gleinalm mountain range, however, is also more complete than those from the Seckauer Tauern. The question arises whether the Seckau and the Gleinalm domains of the Silvretta-Seckau Nappe System represent a continous nappe sheet or two independent parts with a prominent shear zone in between which decoupled them during their exhumation. Based on mapping no major fault is known yet which could have caused the decoupling, until the sinistral Mur-Mürz fault developed during lateral extrusion of the Eastern Alps (Ratschbacher et al., 1991) during Miocene times. If this is the case the Seckau Complex was a south dipping element from Cretaceous until Paleogene time when extensional tectonics and/or pronounced erosion in the south caused a tilting in a more horizontal position.

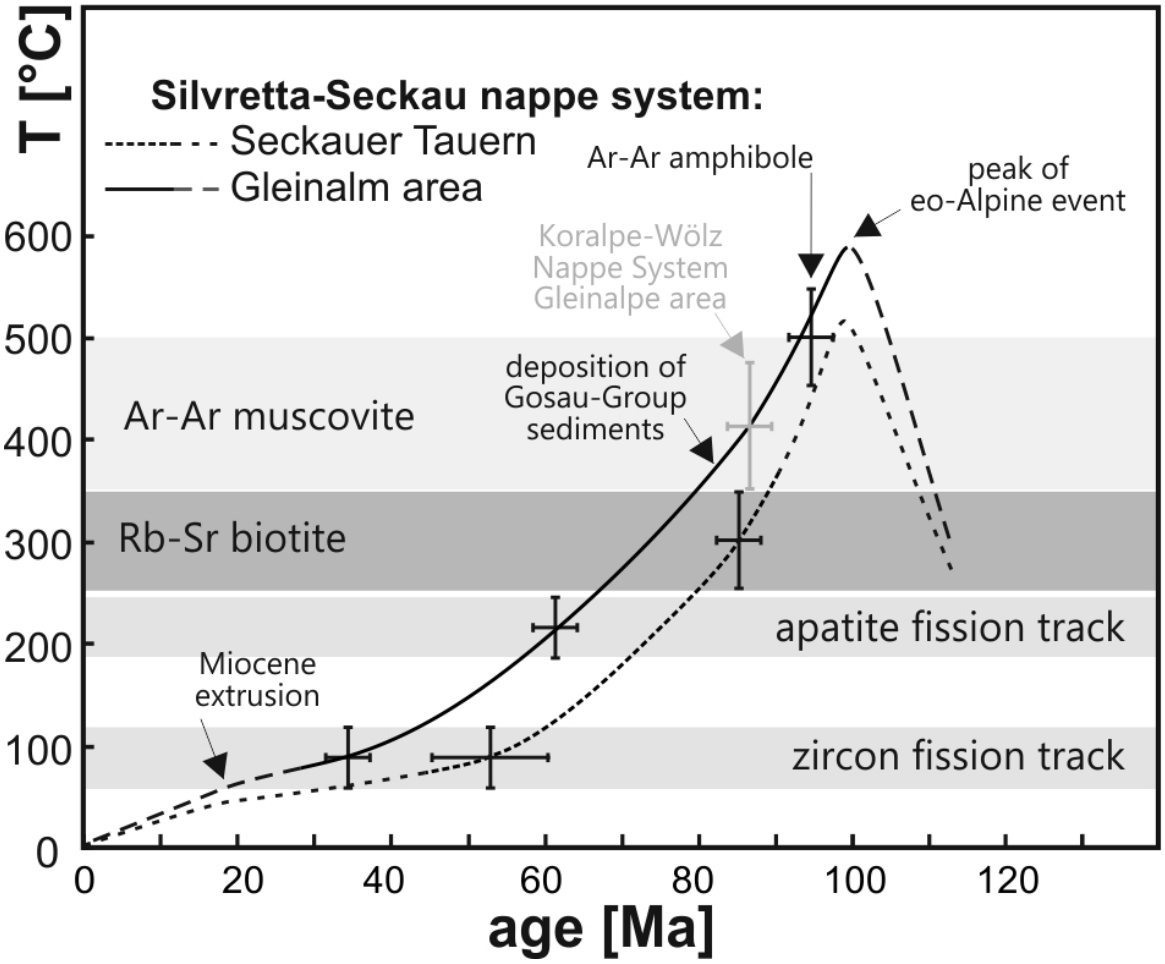

Figure 7: T-t paths for the different parts of the Seckau nappe: Rocks from Seckauer Tauern experienced eo-Alpine peak conditions and cooled earlier than those from the Gleinalm area. Diagram based on data from Dunkl et al. (2005), Faryad and Hoinkes (2001, 2003), Hejl (1997), Neubauer et al. (1995) and Scharbert (1981). For explanation see text.

Description of Stops

Site 1: Migmatized basement of the Seckau Complex

Locality: Steinmühle near Seckau (47°15'51"N; 14°45'30"E)

The metapelites (garnet-micaschists, biotite-plagioclase gneisses) of the pre-Alpine (probably pre-Variscan) basement of the Seckau Complex is partly migmatized. The migmatites mainly occur as banded gneisses with mm- to cm- thick layers of quartz, plagioclase, muscovite and biotite, and with blasts of garnet.

At this site, the migmatitic layering and the penetrative foliation is affected by tight folding with an approximately E-W- trending, subhorizontal fold axis (Fig. 8). The fold axis is sub-parallel to the stretching lineation. Pegmatite dykes that crosscut the migmatic layering are partly affected by folding (Fig. 9). Some pegmatite dykes, however, remain unfolded. All these fabrics are subsequently affected by open folds at a scale of several meters. The related fold axis is subparallel to the stretching lineation, too.

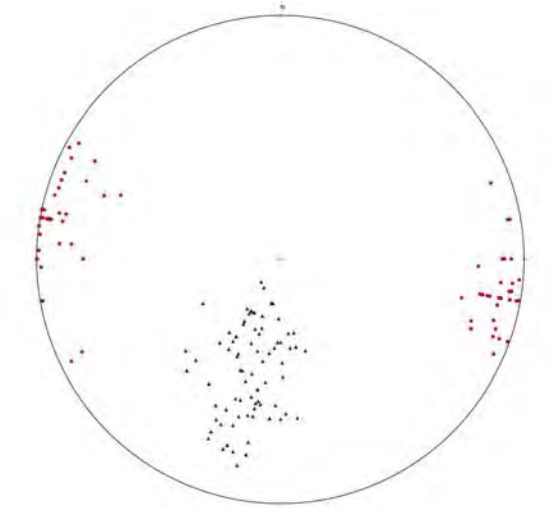

Figure 8: Orientation data of the penetrative foliation (circles, 92 data) and stretching lineation (red dots, 84 data) from paragneisses, micaschists and migmatite gneisses at site 4. The poles to the foliation form a girdle distribution that indicates folding around an E-W trending axis. Lower hemisphere, equal area plot.

Figure 9: Panoramic view of site 1

Site 2: Grandiorite Gneiss, intruded by pegmatite dyke

Locality: Vorwitzbach (47°17'57"N; 14°41'49"E)

At this site a granite gneiss is discordantly crosscut by a pegmatite dyke. Both are subsequently displaced along a subhorizontal faults zone with SE- directed displacement.
The rock forming mineralogical composition of the granite gneiss is K-Feldspar, bioitite, plagioclase and quartz, with subordinate contents of muscovite and biotite. Myrmekite textures are common. The pegmatites are mainly composed of quartz, K-feldspar and biotite and muscovite.
Following the classification by Middlemost (1994) by application of the TAS diagram for plutonic rocks a sample (SP62) taken from this site is classified as granite. Geochemically, it can be classified as I-type granite with respect to Chappel and White (1974, 2001) (Pfingstl 2013) (Table 1).
A Rb-Sr biotite – whole rock isochron from this site indicates an age of 84.8 Ma (Fig. 5).

Site 3: Paragneisses and micaschists of the Seckau Complex

Locality: Gaal, Roßbachgraben (47°17'07,50"N; 14°33'45"E)

The metapelites of the Seckau complex are highly variable. The lithologies range from biotite-rich (garnet-) micaschists to quartz- and plagioclase- rich paragneisses.
The mineral assemblage within the garnet- micaschists is characterized by quartz, plagioclase, biotite, chlorite and garnet. Commonly, biotite occurs along the penetrative folitaion and within strain shadows around garnet. Both garnet and biotite show retrogression to chlorite (Fig. 10).
Additionally, biotite and/or chlorite chlorite occur as clasts of several millimeters in size, and are asymmetrically deformed to micafish, indicating a top-to-the west sense of shear (Fig. 11). Biotite and chlorite are arranged along shear bands as well and define an extensional crenulation cleavage that indicated top-to-the west sense of shear, too (Fig. 12).
Layers of meta-conglomerates are locally embedded within the micaschist. The thickness of these layers varies from a few decimeters to meters. Quartz pebbles within the meta-conglomerates have grain sizes of a few millimeters up to 5 centimeters and show a strong shape preferred orientation parallel to the penetrative foliation.

Site 4: Granite intrusion

Locality: Rosenkogel (47°17'38"N; 14°33'06,50"E; ca. 1810 m)

The fine-grained micaschists at this site show variable contents of quartz within distinct layers spaced at cm- to dm- scale. The penetrative foliation is gently dipping towards the north to northeast. The micaschists are intruded by coarse grained granites, with K-feldspar up to 5 cm in size. The granites hardly show an internal deformational fabric. The granites are exposed for several tens of meters up to the top of the Rosenkogel (1918 m).

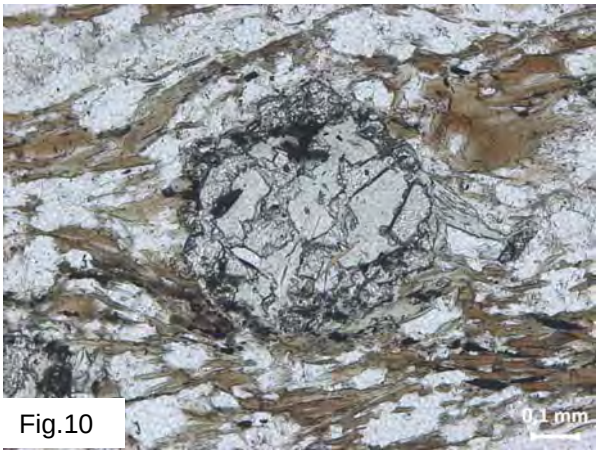

Fig.10

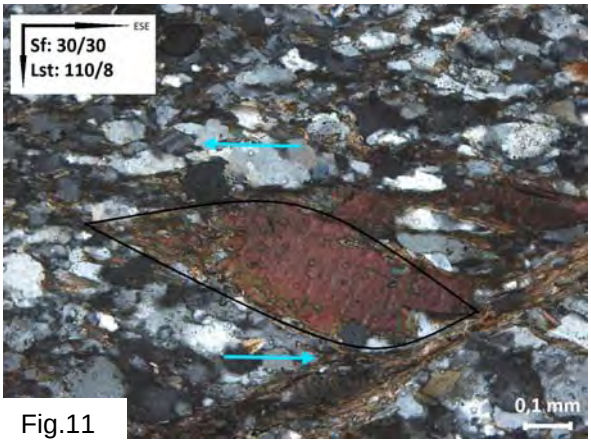

Fig.11

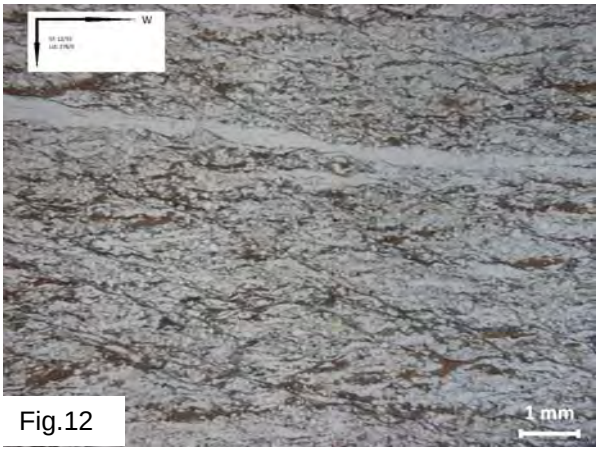

Fig.12

Figure 10: Microtexture of garnet micaschist from the Seckau basement, close to site 3. Biotite formed within strain shadows around garnet, garnet and biotite are transformed to chlorite.

Figure 11: Biotite micafish within garnet micaschist indicating top-to-the west sense of shear.

Figure 12: Extensional crenulation cleavage within garnet micaschist indicating top-to-the west sense of shear.

Appendix

Table 1: Sites of samples analysed for Rb-Sr geochronology on biotite.

Sample	Latitute	Longitude	Altitude (m)	type	Lithology
SP53	47°21.383'	14°47.201'	1455	S-type	granite gneiss; slightly foliated
SP54	47°21.383'	14°47.201'	1455	S-type	orthogneiss. coarse grained
SP56	47°21.450'	14°47.429'	1443	S-type	granodiorite
SP58	47°20.940'	14°48.544'	1482	I-type	granodiorite
SP59	47°20.940'	14°48.544'	1482	I-type	monzodiorite
SP60	47°21.093'	14°48.143'	1447		basic dike
SP62	47°18.016'	14°41.856'	1145	S-type	granite gneiss, coarse grained; migmatic
SP79	47°21.811'	14°40.899'	2416	S-type	granite gneiss
SP80	47°19.695'	14°37.436'	1989	I-type	granodiorite gneiss
SP81	47°19.571'	14°37.657'	2038	I-type	granodiorite gneiss

Table 2: Results of Rb-Sr analysis.

Sample	Material	Rb [ppm]	Sr [ppm]	87Rb/86Sr	87Sr/86Sr	2Sd(m)	age
SP53	WR	108.1	168.3	1.8612	0.714706	0.000004	86.4 ± 0.9
	Bt	628.2	31.48	58.163	0.782542	0.000005	
SP54	WR	90.93	317.5	0.8290	0.710423	0.000004	85.4 ± 0.8
	Bt	535.0	18.40	84.986	0.810618	0.000005	
SP56	WR	100.8	267.3	1.0924	0.712816	0.000004	85.3 ± 0.8
	Bt	438.5	5.442	239.79	0.996507	0.000006	
SP58	WR	72.97	470.4	0.4490	0.708325	0.000004	84.9 ± 0.8
	Bt	356.1	7.182	145.92	0.880531	0.000005	
SP59	WR	74.66	539.5	0.4005	0.708124	0.000004	83.7 ± 0.8
	Bt	287.1	6.571	128.27	0.857332	0.000004	
SP60	WR	78.78	945.7	0.2411	0.706782	0.000004	85.3 ± 0.8
	Bt	298.9	10.19	85.705	0.807810	0.000008	
SP62	WR	118.8	130.4	2.6421	0.724216	0.000004	84.8 ± 0.8
	Bt	619.9	1.194	1815.0	2.837138	0.000015	
SP79	WR	121.9	86.14	4.1077	0.735010	0.000004	80.6 ± 0.8
	Bt	680.1	7.168	283.76	1.049251	0.000006	
SP80	WR	74.69	549.5	0.3934	0.707748	0.000004	76.3 ± 0.8
	Bt	401.5	5.531	214.73	0.935750	0.000005	
SP81	WR	89.93	647.0	0.4022	0.707143	0.000004	84.3 ± 0.8
	Bt	452.5	5.280	255.25	1.006528	0.000006	

Table 3: Chemical composition of selected rocks from Untere Bodenhütte area (SP53-SP78). Ingering Gaal (SP62-SP81). and a mafic dike from Feistritz valley

Sample	SP53	SP54	SP56	SP58	SP59	SP78	SP62	SP79	SP80	SP81	SP60
Petrology	Orthogneiss	Orthogneiss	Orthogneiss	Porph. Granitoid	Porph. Granitoid	Ms-orthogneiss	Bt-orthogneiss*	Bt-orthogneiss*	Bt-orthogneiss	Bt-orthogneiss	Mafic dike
SiO2	70.30	68.45	64.48	63.58	59.14	74.76	69.22	71.24	65.54	63.96	54.41
TiO2	0.38	0.50	0.73	0.84	1.01	0.21	0.45	0.39	0.66	0.70	1.20
Al2O3	14.83	15.25	16.18	16.19	17.06	13.08	15.31	14.00	15.57	16.41	18.07
Fe2O3	2.40	3.27	5.55	5.04	6.47	2.12	3.24	2.85	4.13	4.34	7.52
MnO	0.038	0.055	0.111	0.074	0.127	0.026	0.058	0.047	0.085	0.072	0.139
MgO	0.98	1.04	2.11	1.38	2.58	0.36	0.97	0.72	1.60	1.66	3.40
CaO	1.24	2.03	2.25	3.65	4.89	0.25	1.69	0.95	2.95	3.66	6.30
Na2O	4.14	4.06	3.59	3.41	3.58	3.47	3.55	3.46	4.44	4.15	3.57
K2O	2.86	2.73	2.35	2.95	2.45	3.35	3.44	4.03	2.56	2.57	2.69
P2O5	0.166	0.215	0.124	0.378	0.321	0.123	0.092	0.152	0.231	0.246	0.544
LOI	1.61	1.10	1.60	1.23	1.13	1.04	0.73	1.13	0.82	1.03	0.87
Sum	99.09	98.95	99.28	99.05	99.02	98.93	98.94	99.14	98.85	99.03	99.03
Ba	650	902	478	1454	852	349	558	706	1108	925	1187
Ce	62	83	61	126	95	64	53	73	82	102	157
Cr	<20	<20	48	<20	<20	<20	<20	<20	<20	<20	<20
Cu	<20	<20	<20	<20	<20	<20	<20	<20	<20	<20	<20
Ga	20	21	20	25	21	15	21	19	18	23	23
Nb	<20	<20	<20	<20	<20	<20	<20	26	<20	<20	<20
Nd	50	34	25	54	58	25	35	47	48	41	60
Ni	<20	<20	<20	<20	<20	<20	<20	<20	<20	<20	<20
Pb	<20	<20	32	<20	<20	<20	<20	<20	<20	<20	26
Rb	107	94	105	74	77	141	123	123	75	84	78
Sr	164	308	262	455	522	58	128	82	531	640	911
V	37	49	98	85	139	<20	41	35	73	75	155
Y	20	19	24	18	27	32	33	50	25	25	33
Zn	28	53	109	71	82	23	54	30	84	77	105
Zr	166	209	160	308	224	110	166	262	216	223	271

* S-type affinity

References

Becker, L.P., 1979. Erläuterungen zu Blatt 162 Köflach. - Geologische Karte der Republik

Becker, L.P., 1979. Geologische Karte der Republik Österreich 1:50.000, Blatt 162 Köflach. Geologische Bundesanstalt, Wien.

Chappell B. W., White A. J. R., 2001. Two contrasting granite types: 25 years later. Australian Journal of Earth Sciences, 48, 489–499.

Chappell B. W., White A. J. R., 1974. Two contrasting granite types. Pacific Geology, 8, 173–174.

Dal Piaz, G. V., Martin, S., Villa, I. M., Gosso, G., Marschalko, R., 1995. Late Jurassic blueschist facies pebbles from the Western Carpathian orogenic wedge and paleostructural implications for western Tethys evolution. Tectonics, 14, 874-885..

Dallmeyer, R. D., Neubauer, F., Fritz, H., 2008. The Meliata suture in the Carpathians: regional significance and implications for the evolution of high-pressure wedges within collisional orogens. Geological Society, London, Special Publications, 298, 101-115.

Dunkl, I., Kuhlemann, J., Reinecker, J., Frisch, W., 2005. Cenozoic relief evolution of the Eastern Alps - Contraints from apatite fission track age-provenance of Neogene intramontane sediments. Austrian Journal of Earth Sciences (Mitteilungen der Österreichischen Geologischen Gesellschaft), 98, 92-105.

Faupl, P., Wagreich, M., 2000. Late Jurassic to Eocene Palaeogeography and Geodynamic Evolution of the Eastern Alps. Mitt. Österr. Geol. Ges., 92, 79-94.

Faryad, S. W., Hoinkes, G., 2001. Alpine Chloritoid and Garnet from the Hochgrössen Massif (Speik Complex, Eastern Alps). Mitt. Österr. Mineral. Ges., 146, 387-396.

Faryad, S. W., Hoinkes, G., 2003. P-T gradient of Eo-Alpine metamorphism within the Austroalpine basement units east of the Tauern Window (Austria). Mineralogy and Petrology, 77, 129-159.

Faryad, S.W., Melcher, F.; Hoinkes, G., Puhl, J., Meisel, T., Frank, W., 2002. Relics of eclogite facies metamorphism in the Austroalpine basement, Hochgrössen (Speik complex), Austria. Mineralogy and Petrology, 74, 49-73.

Flügel, H. W.,Neubauer, F. R., 1984. Geologische Karte der Steiermark 1:200.000. Geologische Bundesanstalt, Wien.

Frank, W., 1987. Evolution of the Austroalpine elements in the Cretaceous. In: Flügel, H. W., Faupl, P. Geodynamics of the Eastern Alps. 379-406. Vienna, Deuticke.

Frisch, W., Gawlick, H.-J., 2003.The nappe structure of the central Northern Calcareous Alps and its disintegration during Miocene tectonic extrusion - a contribution to understanding the orogenic evolution of teh Eastern Alps. Int. J. Earth Sci., 92, 712-727.

Froitzheim, N., Plasienka, D., Schuster, R., 2008. Alpine tectonics of the Alps and Western Carpathians. In: McCann, T. The Geology of Central Europe. Volume 2: Mesozoic and Cenozoic. 1141-1232.

Froitzheim, N., Schmid, S. M., Frey, M., 1996. Mesozoic paleogeography and the timing of eclogite facies metamorphism in the Alps: A working hypothesis. Eclogae geol. Helv., 89, 81-110.

Green II, H. W., Dobrzhinetskaya, L., Riggs, E. M., Jin, Z. M., 1997. Alpe Arami: a peridodite massif from the Mantle Transition Zone? Tectonophysics, 279, 1-21.

Hames, W. E., Browning, S. A., 1994. An empirical evaluation of the argon diffusion geometry in muscovite. Earth Planet. Sci. Lett., 124, 161-167.

Hames, W. E., Cheney, J. T., 1997. On the loss of 40Ar* from muscovite during polymetamorphism. Geochim. Cosmochim. Acta, 61, 3863-3872.

Hammerschmidt, K., Frank, E., 1991. Relics of high pressure metamorphism in the Lepontine Alps (Switzerland) - 40Ar/39Ar and microprobe analyses on K-micas. Schweiz. mineral. petrogr. Mitt., 71, 261-274.

Handy, M. R., Oberhänsli, R., 2004. Explanatory notes to the map: metamorphic structure of the Alps: age map of the metamorphic structure of the Alps - tectonic interpretation and outstanding problems. Mitt. Österr. Min. Ges., 149, 201-225.

Hejl, E., 1997. 'Cold spots' during the Cenozoic evolution of the Eastern Alps: thermochronological interpretation of apatite fission-track data. Tectonophysics, 272, 159-173.

Hoinkes, G., Koller, F., Demeny, A., Miller, CH., Schuster, R., Thöni, M., Kurz, W., Krenn, K., Walter, F., 2010. Metamorphism in the Eastern Alps.- Acta Mineralogica-Petrographica, Field Guide Series, 1, 1-47,

Jäger, E., 1979. Introduction to Geochronology. In: Jäger, E., Hunziger, J.C. (Eds): Lectures in Isotopegeology, 1-12, Springer, Berlin Heidelberg New York.

Kirschner, D. L., Cosca, M. A., Masson, H., Hunziker, J. C., 1996. Staircase 40Ar/39Ar of fine-grained white mica: Timing and duration of deformation and empirical constraints on Argon diffusion. Geology, 24, 747-750.

Ludwig, K.R., 2001. Isoplot/Ex rev.2.49: A Geochronological Toolkit for Microsoft Excel. - Berkeley Geochronology Center Special Publication N0. 1a.

Ludwig, K.R., 2003. Isoplot/Ex version 3.0. A geochronological toolkit for Microsoft Excel. Berkeley Geochronological Centre Special Publication, Berkeley, 70 p.

Metz, K., 1967. Geologische Karte der Republik Österreich 1:50.000, Blatt 130-131 Oberzeiring-Kalwang. Geologische Bundesanstalt, Wien.

Metz, K., 1976. Der geologische Bau der Seckauer und Rottenmanner Tauern. Jahrb. Geol. B.-A., 119, 151-205.

Metz, K., 1976. Der geologische Bau der Wölzer Tauern. Mitt. Naturwiss. Ver. Steiermark, 106, 51-75.

Metz, K., 1979. Geologische Karte der Republik Österreich 1:50.000, Blatt 129 Donnersbach. Geologische Bundesanstalt, Wien.

Middlemost, E. A. K., 1994. Naming materials in magma/igneous rock system. Earth Sci. Rev., 37, 215-224.

Missoni, S., Gawlick, H.-J., 2010. Evidence for Jurassic subduction from the Northern Calcareous Alps (Berchtesgaden; Austroalpine, Germany). Int. J. Earth. Sci (Geol. Rundsch.), DOI 10.1007/s00531-010-0552-z.

Nagel, T., 2006. Structure of Austroalpine and Penninic units in the Tilisuna area (Eastern Rhätikon, Austria): Implications for the paleogeographic position of the Allgäu and Lechtal nappes. Eclogae.geol. Helv., 99, 223-235.

Neubauer, F., 1988. Bau und Entwicklungsgeschichte des Rennfeld-Mugel- und des Gleinalm-Kristallins (Ostalpen). Abh. Geol. B.-A., 42, 1-137.

Neubauer, F., 1994. Kontinentkollision in den Ostalpen. Geowissenschaften, 12, 136-140.

Neubauer, F., 2002. Evolution of late Neoproterozoic to early Paleozoic tectonic elements in Central and Southeast European Alpine mountain belts: review and synthesis. Tectonophysics, 352, 87-103.

Neubauer, F., Dallmeyer, R. D., Dunkl, I., Schirnik, D., 1995. Late Cretaceous exhumation of the metamorphic Gleinalm dome, Eastern Alps: kinematics, cooling history and sedimentary response in a sinistral wrench corridor. Tectonophysics, 242, 79-98.

Neubauer, F., Genser, J., Handler, R., 2000. The Eastern Alps: Result of a two-stage collision process. - Mitt. Österr. Geol. Ges., 92. 117-134.

Neubauer, F., Hoinkes, G., Sassi, F.P., Handler, R., Höck, V., Koller, F., Frank, W., 1999. Pre-Alpine metamorphism in the Eastern Alps. – Schweiz. Mineral. Petrogr. Mitt., 79. 41-62, Zürich.

Nowotny, A., Pestal, G., Rockenschaub, M.J., 1993. Die Landecker Quarzphyllit- und Phyllitgneiszone als schwächer metamorpher Anteil des Silvrettakristallins. - Jb. Geol. B.-A., 135, 867-872, Wien.

Pfingstl, S., 2013. Tektonische und metamorphe Entwicklung des Seckauer Kristallins.- Masterarbeit, Naturwisenschaftliche Fakultät, Universität Graz, 121 pp.

Plasienka, D., 1995. Passive and active margin history of the northern Tatricum (Western Carpathians, Slovakia). Geol. Rundsch., 84, 746-760.

Ratschbacher, L., Frisch, W., Neubauer, F., Schmid, S. M., Neugebauer, J., 1989. Extension in compressional orogenic belts. The eastern Alps. Geology, 17, 404-407.

Ratschbacher, L., Frisch, W., Linzer, H.-G., Merle, O., 1991. Lateral Extrusion in the Eastern Alps. Part 2: Structural Analysis. Tectonics, 10, 257-271.

Scharbert, S., 1981. Untersuchungen zum Alter des Seckauer Kristallins. Mitt. Ges. Geol. Bergbaustud. Österr., 27, 173-188.

Schermaier, A., Haunschmid, B., Finger, F., 1997. Distribution of Variscan I- and S-type granites in the Eastern Alps. a possible clue to unravel pre-Alpine basement structures. Tectonophysics, 272, 315-333.

Schmid, S. M., Bernoulli, D., Fügenschuh, B., Matenco, L., Schefer, S., Schuster, R., Tischler, M., Ustaszewski, K., 2008. The Alpine-Carpathian-Dinaric orogenic system: correlation and evolution of tectonic units. Swiss Journal of Geosciences, 101, 139-183.

Schmid, S. M., Fügenschuh, B., Kissling, E., Schuster, R., 2004. Tectonic map and overall architecture of the Alpine orogen. Eclogae geol. Helv., 97 , 93-117.

Schnabel, W., 1980. Permomesozoikum in den zentralen Ostalpen: Zentralalpin (Mittelostalpin), Oberostalpin incl. Zentralalpine Gosau mit Eozän, mittlerer und östlicher Teil (Abb.). In: Oberhauser, R. (Ed.): Der geologische Aufbau Österreichs. Springer Verlag, Wien New York, 406-407.

Schubert, G., Berka, R., Philippitsch, R. 2009. Karte der trinkbaren Tiefengrundwässer Österreichs 1:500.000 In: Arbeitstagung 2007 der Geologischen Bundesanstalt Blatt 67 Grünau im Almtal und Blatt 47 Ried im Innkreis: Linz, 7. - 11. Mai 2007

Schuster, R., Koller, F., Hoeck, V., Hoinkes, G., Bousquet, R., 2004. Explanatory notes to the map: Metamorphic structure of the Alps - Metamorphic evolution of the Eastern Alps. - Mitt. Österr. Miner. Ges., 149, 175-199.

Stüwe, K., Schuster, R., 2010. Initiation of Subduction in the Alps: Continent or Ocean? - Geology 38, 175-178, doi: 10.1130/G30528.

Thöni, M., Jagoutz, E., 1992. Some new aspects of dating eclogites in orogenic belts: Sm-Nd, Rb-Sr and Pb-Pb isotopic results from the Austroalpine Saualpe and Koralpe type-locality (Carinthia/Styria, SE Austria). Geochim. Cosmochim. Acta, 56, 347-368.

Thöni, M., Jagoutz, E., 1993. Isotopic constraints for eo-Alpine high-P metamorphism in the Austroalpine nappes of the Eastern alps: bearing on Alpine orogenesis. Schweiz. mineral. petrogr. Mitt., 73, 177-189.

Thöni, M., Miller, C., Blichert-Toft, J., Whitehouse, M. J., Konzett, J., Zanetti, A., 2008. Timing of high-pressure metamorphism and exhumation of the eclogite type-locality (Kupplerbrunn-Prickler Halt, Saualpe, south-eastern Austria): constraints from correlations of the Sm-Nd, Lu-Hf, U-Pb and Rb-Sr isotopic systems. J. metamorphic Geol., 26, 561-581.

Tollmann, A., 1977. Geologie von Österreich. Band 1. Die Zentralalpen. 766 pp, Deuticke, Wien.

von Blanckenburg, F.,Villa, I.M., 1988. Argon retentivity and argon excess in amphiboles from the garbenschists of the Western Tauern Window, Eastern Alps. Contrib. Mineral. Petrol., 100, 1-11.

von Blanckenburg,F., Villa,I.M., Baur,H., Morteani,G., Steiger,R.H., 1989. Time Calibration of a PT-path from the Western Tauern Window, Eastern Alps: the problem of closure temperatures. Contrib. Mineral. Petrol., 101, 1-11.

Wölfler, A., Kurz, W., Danisik, M., Rabitsch, R., 2010 Dating of fault zone activity by apatite fission track and apatite (U-Th)/He thermochronometry: a case study from the Lavanttal fault system (Eastern Alps). Terra Nova, 22, 274-282.

Wolf, R. A., Farley, K. A., Silver, L. T., 1996. Helium diffusion and low temperature thermochronometry of apatite. Geochim. Cosmochim. Acta, 60, 4231-4240.